Inorg. Chem. **2006**, *45*, 4277−4283

EPR and UV−Vis Studies of the Nitric Oxide Adducts of Bacterial Phenylalanine Hydroxylase: Effects of Cofactor and Substrate on the Iron Environment

Andrew Y. Han, Amanda Q. Lee, and Mahdi M. Abu-Omar*

Brown Laboratory, Department of Chemistry, Purdue University, 560 Oval Drive, West Lafayette, Indiana 47907

Received March 21, 2006

Phenylalanine hydroxylase from *Chromobacterium violaceum* (cPAH), which catalyzes phenylalanine oxidation to tyrosine, is homologous to the catalytic domain of eukaryotic PAHs. Previous crystallographic and spectroscopic studies on mammalian PAH conflict on whether O_2 binds to the open-coordination site or displaces the remaining water ligand to yield either a six- or a five-coordinate iron, respectively. The abilities of nitric oxide to behave as an oxygen mimic and a spectroscopic probe of ferrous iron are used to investigate the geometric and electronic effects of cofactor and substrate binding to cPAH by electron paramagnetic resonance (EPR) and UV−vis spectroscopies. A rhombic distortion observed for the ternary complex is due to two factors: a decrease in the Fe−NO angle and an alteration in the equatorial ligand geometry. Both factors are consistent with NO displacing the sole remaining water ligand to yield a five-coordinate iron center. Hyperfine broadening of the EPR resonances of the nitrosyl complexes by ^{17}O-enriched water is observed in the absence of substrates or presence of cofactor only (binary complex), demonstrating that water is bound to the Fe^{II}. However, in the presence of substrate and cofactor (ternary complex), the EPR resonances of the nitrosyl complex are not broadened by ^{17}O-enriched water, indicating the displacement of water by NO to afford a five-coordinate iron. Furthermore, the increased intensity in the 500–600 nm range of the UV−vis spectrum of the ternary nitrosyl complex indicates an increased overlap between the in-plane NO $2\pi^*$ and $d_{x^2-y^2}$ and d_{xz} orbitals, which corroborates a five-coordinate iron.

Introduction

Phenylalanine hydroxylase (PAH) is a non-heme iron-dependent monooxygenase that activates molecular oxygen in order to catalyze the oxidation of phenylalanine to tyrosine. Reduced tetrahydrobiopterin (BH_4) cofactor acts as the source of electrons and is subsequently oxidized to the dihydrobiopterin form (BH_2; Scheme 1).[1,2] Because this enzyme represents the rate-determining step in the catabolic pathway of phenylalanine, defects in its activity may lead to the metabolic disorder phenylketonuria, which causes irreversible mental retardation during childhood development.[3] PAH belongs to a family of pterin-dependent aromatic amino acid hydroxylases (AAAHs), which includes tyrosine and tryptophan hydroxylase. The mammalian AAAHs comprise three functional domains: an N-terminal regulatory domain, a C-terminal oligomerization domain, and a catalytic domain

Scheme 1. Reaction Catalyzed by Phenylalanine Hydroxylase (PAH)

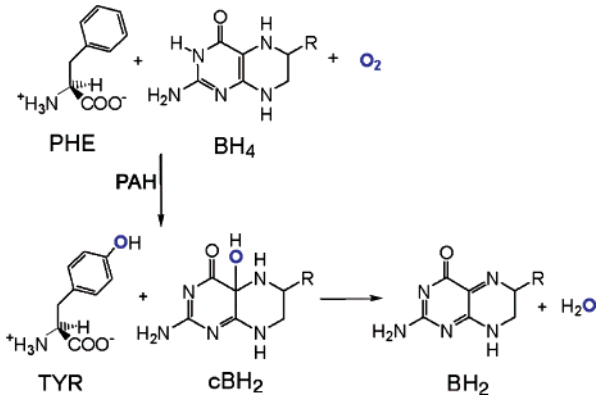

* To whom correspondence should be addressed. E-mail: mabuomar@purdue.edu. Fax: (765) 494-0239.

(1) Solomon, E. I.; Brunold, T. C.; Davis, M. I.; Kemsley, J. N.; Lee, S.-K.; Lehnert, N.; Neese, F.; Skulan, A. J.; Yang, Y.-S.; Zhou, J. *Chem. Rev.* **2000**, *100*, 235−349.
(2) (a) Fitzpatrick, P. F. *Biochemistry* **2003**, *42*, 14083−14091. (b) Abu-Omar, M. M.; Loaiza, A.; Hontzeas, N. *Chem. Rev.* **2005**, *105*, 2227−2252.
(3) Kappock, T. J.; Caradonna, J. P. *Chem. Rev.* **1996**, *96*, 2659−2756.

10.1021/ic060478p CCC: $33.50
Published on Web 04/14/2006

that possesses one glutamate and two histidine side chains that serve as the iron ligands. Bacterial PAH, which consists of only one domain and exists as a monomer, shares a modest degree of homology (~35%) with this catalytic domain in mammalian AAAHs. Furthermore, comparison of the crystal structures of bacterial PAH from *C. violaceum* (cPAH) and human PAH (hPAH) have shown that both exhibit similar folds.[4] Therefore, cPAH, which, in contrast to mammalian PAH, is readily expressed and purified in large, soluble quantities, serves as a facile model for the more-complex mammalian form. For example, the lack of a regulatory domain in cPAH has proven to be useful in determining the steady-state kinetic mechanism for this enzyme, which follows an ordered binding mechanism: $DMPH_4$ (6,7-dimethyltetrahydropterin) + Phe + O_2.[5] Although an unambiguous kinetic mechanism has yet to be established for mammalian PAH, current data strongly suggest an ordered sequential mechanism: Phe + BH_4 + O_2.[3,6]

To understand how PAH controls the substrate binding order, which ensures that hydroxylation of phenylalanine and oxidation of the pterin cofactor are coupled, researchers have performed a large amount of spectroscopic and crystallographic studies. Spectroscopic studies on the ferrous iron active site of rPAH (rat) by Solomon and co-workers have revealed that in the iron center, which possesses a distorted octahedral geometry for the native enzyme (without cofactor and substrate present), the cofactor-bound and phenylalanine-bound forms lose a water ligand and assume a five-coordinate, square-pyramidal geometry when both cofactor and substrate are present.[7−9] This observed change in ligand geometry was further supported by the crystal structure of truncated, ferrous hPAH, which revealed a distorted, square-pyramidal geometry for the ternary complex of hPAH, BH_4, and a Phe analogue.[10] Dioxygen binding is proposed to occur at the open-coordination site to yield a six-coordinate iron center, a mechanism shared with non-heme, α-ketoacid-dependent hydroxylases and the extradiol dioxygenases.[11] However, modeling studies on the ternary hPAH crystal structure have suggested that dioxygen would displace the remaining water ligand rather than bind to the open-coordination site, as positioning of dioxygen to the latter would be sterically hindered by the O4 oxygen atom on BH_4 and would place the proximal oxygen atom of dioxygen ~2 Å farther from the phenylalanine substrate.[10] Obviously, further experiments are needed to resolve this discrepancy.

The catalytically relevant ferrous state of cPAH lacks electronic transitions in the UV−visible region and possesses an $S = 2$ spin state, which makes it inaccessible by conventional EPR (electron paramagnetic resonance) methods. However, the nitric oxide adduct of ferrous, high-spin iron proteins exhibits both ligand-to-metal charge-transfer transitions in the visible region between the NO and metal orbitals and an $S = {}^3/_2$ spin state, detectable by EPR.[12] These properties have proven to be advantageous in the study of a number of heme and non-heme iron metalloproteins.[13−18] Additionally, nitric oxide behaves as a surrogate for dioxygen, with the NO adduct of oxygen-activating iron enzymes serving as a valuable model of the oxygen-bound intermediate prior to cleavage of the oxygen−oxygen bond. Herein, we report on how the iron geometry of ferrous cPAH affects the nitric oxide binding ability of the iron center by electron paramagnetic resonance (EPR) and electronic absorption spectroscopy. More specifically, by exploiting these spectroscopic and oxygen-mimicking properties of nitric oxide and hyperfine broadening in ^{17}O-enriched water, we determined that the presence of both cofactor and substrate induces a change in iron geometry to a five-coordinate species, where nitric oxide displaces the sole water ligand, and that this five-coordinate species binds nitric oxide with increased affinity compared to the free and binary (cPAH−cofactor or cPAH−substrate) forms of the enzyme.

Materials and Methods

L-Phenylalanine, dithiothreitol (DTT), ferrous ammonium sulfate, *N*-(2-hydroxyethyl) piperazine-*N*′-(ethanesulfonic acid) (HEPES), and all other assay reagents were of the highest quality, purchased from Sigma (St. Louis, Mo), and used as received. 6,7-Dimethyl-5,6,7,8-tetrahydropterin ($DMPH_4$) was obtained from Fluka (Milwaukee, WI). Diethylamino NONOate DEA/NO (Diethylammonium (*Z*)-1-(*N*,*N*-diethylamino)diazen-1-ium-1,2-diolate) was synthesized according to published procedures,[19] with higher oxide impurities of NO previously removed from the nitric oxide gas (Matheson) by bubbling through a strong basic solution and subsequent passage through a coldfinger immersed in a slush of dry ice/2-propanol. High-purity nitrogen gas (BOC Gases) was used to purge the diethylamine and diethyl ether solution before the addition of nitric oxide. The purity of synthesized DEA/NO was determined by ^1H NMR and UV−visible spectroscopy before the DEA/NO was stored at −20 °C in a tightly capped glass vial. Results were also reproduced with commercial DEA/NO purchased from Cayman Chemical (Ann Arbor, MI). ^{17}O-enriched water to 60 at % was obtained from Icon Services. Enzyme kinetic assays

(4) Erlandsen, H.; Kim, J. Y.; Patch, M. G.; Han, A.; Volner, A.; Abu-Omar, M. M.; Stevens, R. C. *J. Mol. Biol.* **2002**, *320*, 645−661.
(5) Volner, A.; Zoidakis, J.; Abu-Omar, M. M. *J. Biol. Inorg. Chem.* **2003**, *8*, 121−128.
(6) Xia, T.; Gray, D. W.; Shiman, R. *J. Biol. Chem.* **1994**, *269*, 24657−24665.
(7) Kemsley, J. N.; Zaleski, J. M.; Caradonna, J. P.; Solomon, E. I. *J. Am. Chem. Soc.* **1999**, *121*, 1528−1536.
(8) Loeb, K. E.; Westre, T. E.; Kappock, T. J.; Mitiç, N.; Glasfeld, E.; Caradonna, J. P.; Hedman, B.; Hodgson, K. O.; Solomon, E. I. *J. Am. Chem. Soc.* **1997**, *119*, 1901−1915.
(9) Wasinger, E. C.; Mitic, N.; Hedman, B.; Caradonna, J.; Solomon, E. I.; Hodgson, K. O. *Biochemistry* **2002**, *41*, 6211−6217.
(10) Andersen, O. A.; Flatmark, T.; Hough, E. *J. Mol. Biol.* **2002**, *320*, 1095−1108.
(11) Solomon, E. I.; Decker, A.; Lehnert, N. *Proc. Natl. Acad. Sci. U.S.A.* **2003**, *100*, 3589−3594.
(12) Brown, C. A.; Pavlosky, M. A.; Westre, T. E.; Zhang, Y.; Hedman, B.; Hodgson, K. O.; Solomon, E. I. *J. Am. Chem. Soc.* **1995**, *117*, 715−732.
(13) Chen, V. J.; Orville, A. M.; Harpel, M. R.; Frolik, C. A.; Surerus, K. K.; Münck, E.; Lipscomb, J. D. *J. Biol. Chem.* **1989**, *264*, 21677−21681.
(14) Nelson, M. J. *J. Biol. Chem.* **1987**, *262*, 12137−12142.
(15) Arciero, D. M.; Orville, A. M.; Lipscomb, J. D. *J. Biol. Chem.* **1985**, *260*, 14035−14044.
(16) Jackson, T. A.; Yikilmaz, E.; Miller, A.-F.; Brunold, T. C. *J. Am. Chem. Soc.* **2003**, *125*, 8348−8363.
(17) Hegg, E. L.; Whiting, A. K.; Saari, R. E.; McCracken, J.; Hausinger, R. P.; Que, L., Jr. *Biochemistry* **1999**, *38*, 16714−16726.
(18) Clay, M. D.; Cosper, C. A.; Jenney, F. E., Jr.; Adams, M. W. W.; Johnson, M. K. *Proc. Natl. Acad. Sci. U.S.A.* **2003**, *100*, 3796−3801.
(19) Drago, R. S.; Paulik, F. E. *J. Am. Chem. Soc.* **1960**, *82*, 96−98.

were performed as described previously by monitoring tyrosine production at 275 nm.[5] Matrix-assisted laser desorption mass spectra (MALDI-MS) were acquired on an Applied Biosystems Voyager DE PRO.

Electron Paramagnetic Resonance Spectroscopy. Preparation of EPR samples was carried out in an anaerobic glovebox (VAC systems glovebox with custom-altered dri-train) under argon (<5 ppm oxygen), in which the chamber temperature varied between 33 and 37 °C. Buffer solutions for EPR samples were stored in 60 mL serum vials capped with rubber septa and deoxygenated by bubbling argon gas through them for 2 hours/60 mL. Preweighed amounts of solid L-Phe, $DMPH_4$, DEA/NO, and ferrous ammonium sulfate were placed in separate 1.5 mL microcentrifuge tubes and brought into the glovebox along with a 1 mL aliquot (20−25 mg/mL) of frozen enzyme. L-Phe was dissolved in low-salt buffer (100 mM HEPES, 50 mM NaCl, pH 7.4); both $DMPH_4$ and ferrous ammonium sulfate were dissolved in 10 mM HCl, and DEA/NO was dissolved in 10 mM NaOH. UV−visible spectra, recorded on a Shimadzu UV-2501 double-beam spectrophotometer equipped with a thermostat cell holder, were taken of dilutions of the L-Phe, $DMPH_4$, and DEA/NO stocks; their concentrations were determined from published extinction coefficients.[20] To reconstitute the apoenzyme with ferrous iron, we first facilitated removal of dissolved oxygen by gently pipetting the thawed enzyme solution up and down in the microcentrifuge tube (∼50 repetitions), followed by addition of a small amount of solid sodium dithionite. Ferrous ammonium sulfate solution was added slowly to the enzyme solution to reach a final Fe(II):enzyme concentration of 5:1. To remove the excess Fe(II), we desalted the enzyme sample on a NAP-10 desalting column (Amersham Biosciences), which was previously equilibrated in the glovebox with 50 mL of freshly prepared, deoxygenated sodium dithionite solution in low-salt buffer, followed by equilibration with deoxygenated high-salt buffer (100 mM HEPES, 200 mM NaCl, pH 7.4). The Fe(II)-reconstituted enzyme was eluted with 1.5 mL of high salt buffer and its concentration was determined by UV−visible spectroscopy (A_{280}) using published extinction coefficients.[5] Metal content for reconstituted cPAH samples typically reached 65−85% metalation, as determined by inductively coupled plasma atomic emission (ICP-AE) spectrometry with a Jarrell Ash Series 1000 spectrometer. Appropriate volumes of the ferrous enzyme, Phe, and $DMPH_4$ solutions were added to low-salt buffer in microcentrifuge tubes for a final sample volume of 0.3 mL. DEA/NO solution was added (for a final concentration of 0.5 mM DEA/NO) to each tube and allowed to incubate for 20 min. Each sample was then transferred to EPR tubes (4 mm o.d.), capped, sealed with Parafilm, and immediately frozen in liquid nitrogen after removal from the glovebox. Alternatively, a limiting amount of ferrous ammonium sulfate (25−35 μM) was added to apo-cPAH (50 μM) to reconstitute the enzyme, and other reagents were added as described above. Spin quantitations were performed by double integration of the spin signal due to the iron nitrosyl adduct versus that of Fe^{II}(EDTA)(NO) standards.

Spectra were recorded on a Bruker EMX spectrophotometer equipped with a liquid helium continuous flow cryostat (Oxford Instruments) or a Bruker ESP 300E equipped with an Oxford ESR 900 liquid helium continuous flow cryostat and an Oxford ITC4 temperature system to monitor and regulate the temperature. Spectra were obtained under nonsaturating conditions using 9.4 GHz frequency and 100 kHz field modulation. EPR simulations were performed with the SIMFONIA software package (Bruker).

EPR Spectra in ^{17}O-Enriched Water. Enzyme stock solution (75 μL, 200 μM) was concentrated to 10 μL using a Microcon YM-10 centrifugal filtering device. For a final sample volume of 0.3 mL, appropriate volumes of HEPES buffer made with ^{17}O water were added to the concentrated enzyme solution before ferrous ammonium sulfate, Phe, $DMPH_4$, and then DEA/NO solutions were added. The mixture was allowed to incubate for 20 min. The final concentrations of the reagents were as follows: cPAH, 50 μM; ferrous ammonium sulfate, 25 μM; Phe, 1 mM; $DMPH_4$, 1 mM; and DEA/NO, 500 μM. The final solution contained approximately 53 atom % enrichment of ^{17}O water.

Electronic Absorption Spectroscopy. The buffers, iron-reconstituted enzyme, Phe, $DMPH_4$, and DEA/NO were prepared anaerobically following the procedures used for the EPR samples and combined in a microcentrifuge tube for a total volume of 1 mL, in which the final concentrations were 0.05 mM Fe(II)-reconstituted enzyme, 1 mM Phe and/or $DMPH_4$, and DEA/NO concentrations that varied from 7.5 μM to 1.5 mM. Approximately 0.8 mL of the sample was immediately placed in a semimicro quartz cuvette, sealed with a Teflon stopper, and wrapped in Parafilm. This sample volume was used to minimize the amount of void volume present between the top of the solution and the bottom of the stopper in the cuvette. The cuvette was then incubated for 20 min (∼10 half-lives of DEA/NO at 37 °C) in the glovebox to allow sufficient release of nitric oxide. The amount of NO released per mole of DEA/NO has been shown to be 1.5 mol.[20] A spectrum from 300 to 700 nm was taken immediately after removal of the cuvette from the glovebox. To build the NO binding curves for cPAH in the presence or absence of cofactor and substrate, we determined the extinction coefficients of each complex at saturating NO concentrations (∼2.0 mM). Extinction coefficients at 440 nm (the wavelength at which the spectra of the NO adduct of cPAH with both Phe and $DMPH_4$ bound exhibits a peak) were found to be 1990 ± 70 M^{-1} cm^{-1} for the NO adduct of cPAH−Fe(II) alone, 1970 ± 70 M^{-1} cm^{-1} for the $DMPH_4$-bound complex, 2225 ± 100 M^{-1} cm^{-1} for the Phe-bound complex, and 2300 ± 100 M^{-1} cm^{-1} for the $DMPH_4$- and Phe-bound complex. For each NO binding curve, the extinction coefficient was used to calculate the concentration of ferrous enzyme bound by NO; this concentration was subtracted from the total amount of nitric oxide added initially to the sample (as DEA/NO) to determine the free NO concentration, assuming an insignificant amount of NO equilibrated with the small void volume above the solution.

Results and Discussion

EPR of Nitric Oxide Adducts of Wild-Type cPAH. To monitor the changes to the Fe−NO electronic environment upon substrate and cofactor binding, we performed X-band EPR spectroscopy on samples of the nitrosyl adduct of ferrous-reconstituted cPAH (cPAH−Fe) in the presence or absence of Phe and reduced ($DMPH_4$) or oxidized ($DMPH_2$) cofactor. All of the nitrosyl cPAH−Fe samples exhibited approximately axial $S = {}^3/_2$ EPR signals of g_x, $g_y \approx 4$ and $g_z \approx 2$, consistent with previously studied {Fe−NO}^{7} paramagnetic centers in various non-heme iron(II) oxygenases.[13−18] As described by Solomon et al., the following spin Hamiltonian (eq 1) can be used to analyze EPR spectra for $S = {}^3/_2$ species, where D and E are the axial and rhombic zero-field splitting parameters, respectively.[12]

$$H = D[S_z^2 - S(S+1)/3] - E(S_x^2 - S_y^2) + \gamma o \beta S H \quad (1)$$

(20) Maragos, C. M.; Morley, D.; Wink, D. A.; Dunams, T. M.; Saavedra, J. E.; Hoffman, A.; Bove, A. A.; Issac, L.; Hrabie, J. A.; Keefer, L. K. *J. Med. Chem.* **1991**, *34*, 3242−3247.

Table 1. Summary of EPR Data and NO Dissociation Constants

sample	experimental		simulation parameters			
	g_x, g_y	K_d[a] (μM)	% of population[b]	g_x, g_y, g_z	line width[c] (l_x, l_y, l_z) (G)	E:D
cPAH−Fe•(NO)	4.08, 3.96	210 ± 30	100	4.09, 3.96, 2.00	(29, 31, 32)	0.011
cPAH−Fe•($DMPH_4$)•(NO)	4.06, 3.98	150 ± 10	61	4.06, 3.98, 2.00	(23, 24, 23)	0.007
			39	4.12, 3.92, 2.00	(22, 26, 23)	0.017
cPAH−Fe•($DMPH_2$)•(NO)	4.05, 3.98	n.d.[d]	66	4.06, 3.98, 2.00	(23, 24, 23)	0.007
			34	4.12, 3.92, 2.00	(22, 26, 23)	0.017
cPAH−Fe•(Phe)•(NO)	4.15, 3.89	220 ± 20	100	4.17, 3.90, 2.00	(22, 27, 20)[e]	0.023
cPAH−Fe•($DMPH_4$)•(Phe)•(NO)	4.27, 3.76	31 ± 2	90	4.29, 3.77. 2.00	(33, 48, 20)[e]	0.044
			10	4.15, 3.90, 2.00	(19, 22, 20)[e]	0.022

[a] Dissociation constants measured by UV−visible spectroscopy, as described in the legend of Figure 5 and in Materials and Methods. [b] Percentage of total EPR signal. [c] All line shapes are Lorentzian, unless indicated otherwise. [d] n.d. = not determined. [e] Line shape is a 0.1 Lorentzian:Gaussian mixture.

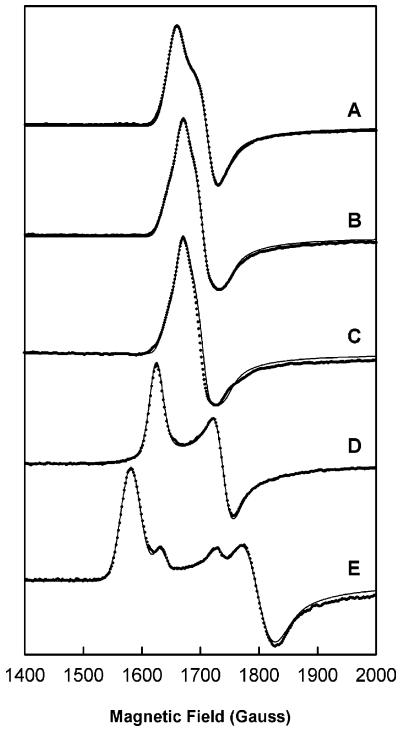

Figure 1. Experimental and simulated EPR spectra of the $g = 4$ region of ferrous nitrosyl cPAH−Fe complexes at 4 K. Each sample contained 50 μM enzyme, 0.5 mM DEA/NO, and substrate and cofactor concentrations of 1 mM, when indicated. (A) cPAH−Fe•(NO); (B) cPAH−Fe•($DMPH_4$)•(NO); (C) cPAH−Fe•($DMPH_2$)•(NO); (D) cPAH−Fe•(Phe)•(NO); (E) cPAH−Fe•($DMPH_4$)•(Phe)•(NO). Experimental spectra are shown as open circles, and black lines indicate simulation trace. Simulation parameters are listed in Table 1.

The E:D ratio reflects the degree of rhombic distortion of the {Fe−NO}^{7} center, with values ranging from 0 for purely axial signals to $^1/_3$ for purely rhombic signals. For systems exhibiting low rhombicity (E:D < 0.15), E:D can be determined from g_x, g_y, and g_z using the following relationships[15]

$$g_x = g_0[2 - 3(E/D) - {}^3/_2(E/D)^2],\ g_y = g_0[2 + 3(E/D) - {}^3/_2(E/D)^2],\ g_z = g_0[1 - 3(E/D)^2] \quad (2)$$

where g_0 is taken to be 2. Because the $g = 2$ signal is obscured by the large signal of free NO, previously observed in frozen buffer solutions of NO,[12] only the more informative $g = 4$ region is shown (Figure 1). A simulation of the EPR signal for the NO adduct of ferrous cPAH, cPAH−Fe•(NO), indicates that this complex exists as a single population (Figure 1, spectrum A, and Table 1). However, simulations for both the oxidized and reduced cofactor-bound nitrosyl complexes, cPAH−Fe•($DMPH_4$)•(NO) and cPAH−Fe•($DMPH_2$)•(NO), respectively, indicate that each of these complexes are composed of two distinct populations: an axial species and a more-rhombic species (Figure 1, spectra B and C, and Table 1). The relative proportions of these axial and rhombic species are similar for both cPAH−Fe•($DMPH_4$)•(NO) and cPAH−Fe•($DMPH_2$)•(NO), with axial:rhombic percent compositions of 61:39 and 66:34, respectively. A greater degree of rhombic distortion occurs with the substrate-bound complex of cPAH−Fe•(Phe)•(NO), simulations of which indicate a single population (Figure 1, spectrum D). Last, the quaternary complex of cPAH−Fe•($DMPH_4$)•(Phe)•(NO) exhibits the largest degree of rhombic distortion of all the complexes, with its major species possessing an E:D of 0.044 and $g_x = 4.29$, $g_y = 3.77$, and $g_z = 2.00$ (Figure 1, spectrum E, and Table 1). This major species accounts for 90% of the EPR signal, whereas the remaining 10% has g values similar to that of cPAH−Fe•(Phe)•(NO).

Spin quantitations of the iron nitrosyl signal accounted for >90% of the iron in the enzyme samples for both reconstituted holo-cPAH and apo-cPAH with limiting added ferrous. Furthermore, enzyme samples used in NO studies exhibited proper activity upon normalization for metal content, and MALDI-MS analyses of cPAH post-treatment with NO (DEA/NO) showed no protein modification. These observations demonstrate reversible binding of NO to iron in the active site of cPAH without affecting the enzyme's integrity.

The heretofore described electronic and geometric changes to the ferrous center of cPAH are qualitatively consistent with previous spectroscopic studies performed on ferrous rPAH and hPAH.[21,22] However, the site of oxygen binding has yet to be determined.

The observed increase in rhombicity for the nitrosyl-cPAH complexes may be attributed to two possible structural changes in the iron ligand environment. The first possibility is that the Fe−N−O angle decreases upon the addition of

(21) Kappock, T. J.; Harkins, P. C.; Friedenberg, S.; Caradonna, J. P. *J. Biol. Chem.* **1995**, *270*, 30532−30544.
(22) Hagedoorn, P.-L.; Schmidt, P. P.; Andersson, K. K.; Hagen, W. R.; Flatmark, T.; Martinez, A. *J. Biol. Chem.* **2001**, *276*, 22850−22856.

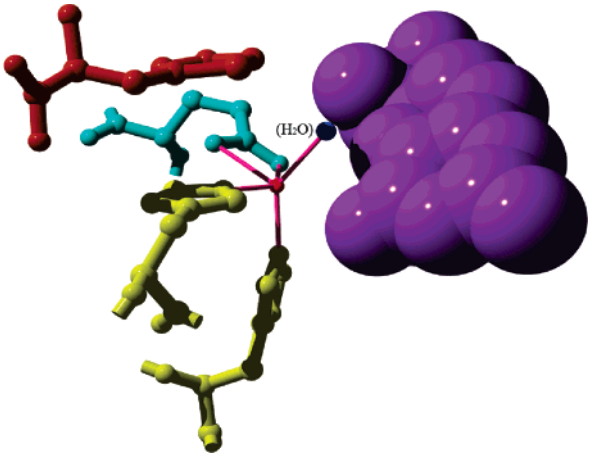

Figure 2. Iron site for human phenylalanine hydroxylase (hPAH), using the ternary crystal structure (PDB ID:1KW0) of ferrous hPAH with bound cofactor (CPK in purple) and phenylalanine substrate analogue 3-(2-thienyl)-L-alanine (THA, shown in orange). The two histidine (yellow) and one glutamate (aqua blue) iron ligands are shown in the ball-and-stick model. The iron center is a red sphere and the water ligand is a blue sphere. This figure was created with the DeepView/Swiss-PdbViewer 3.7 program and Pov-Ray 3.5 programs.

Phe, resulting in the observed increase in rhombicity for the cPAH−Fe·(Phe)·(NO) complex. This reduction in Fe−N−O angle may be exacerbated by the presence of both cofactor and substrate, giving rise to the greater *E*:*D* value for cPAH−Fe·(DMPH$_4$)·(Phe)·(NO). Support for such a model comes from studies on five-coordinate iron nitrosyl complexes by Borovik et al., in which the NO ligand was sterically restricted to increasingly linear geometries, resulting in a decrease in the *E*:*D* value.[23] At some limit, the Fe−N−O angle decreases such that NO becomes bound side-on. This scenario has been observed recently for copper in nitrite reductase.[24] Side-on binding would be more favorable for O_2 than for NO. However, without a molecular structure for the nitrosyl adduct of cPAH, side-on binding of NO cannot be substantiated. Unfortunately, our attempts to obtain X-ray quality single crystals of the nitrosyl adduct of cPAH were not successful.

The second possibility is that the increased rhombicity reflects a distortion in the electronic environment equatorial to the axial Fe−NO bond, because of an increase in bond strength or change in ligand geometry of the equatorial histidine and glutamate ligands. Two examples from the literature are IPNS, in which the creation of a strong Fe−thiolate bond equatorial to the NO ligand increases the *E*:*D* value from 0.015 to 0.035,[13] and the intradiol-cleaving enzyme, protocatechuate 3,4-dioxygenase, in which the presence of both the catecholate substrate and endogenous phenolate equatorial ligands increases the *E*:*D* value from 0.055 to 0.175 for the nitrosyl adduct.[15]

Inspection of the crystal structure of the ternary complex of hPAH (Figure 2) reveals that both factors may contribute to the increased rhombicity of the cPAH structure. The addition of both Phe and cofactor may exacerbate the decrease in the Fe−N−O angle, and the position of the NO ligand would be displaced toward the cofactor if it indeed replaces the remaining water ligand on iron (vide infra). Because NO is used as an oxygen mimic for non-heme enzymes, it is not unreasonable to believe that the enzyme would sterically restrict the conformation of the Fe−NO to that of the substrate oxygen.

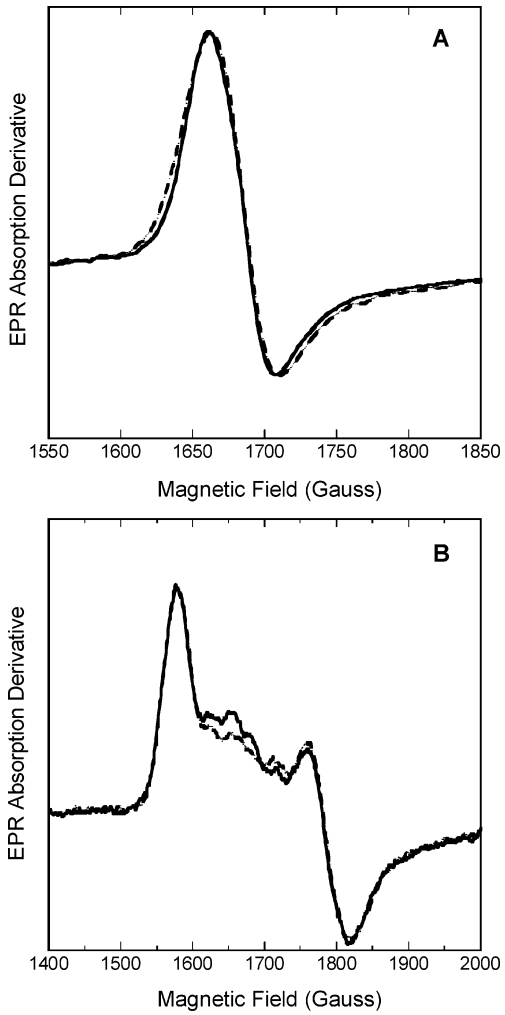

Figure 3. EPR spectra of the $g = 4$ region of ferrous nitrosyl complexes of cPAH in ^{16}O (solid line) and ^{17}O (dashed line) water at 4 K for binary complex (A) cPAH−Fe·(DMPH$_4$)·(NO) and ternary complex (B) cPAH−Fe·(DMPH$_4$)·(Phe)·(NO).

To address the change in ligand geometry on iron, we obtained EPR spectra of cPAH nitrosyl complexes in ^{17}O-enriched water. The native enzyme in the absence of substrates, cPAH−Fe·(NO), and binary complex, cPAH−Fe·(DMPH$_4$)·(NO), results in a 0.4−0.5 mT broadening of the EPR resonances in $^{17}OH_2$ (Figure 3a and Table 2). Transferred hyperfine interaction of this type is observed only when there is a direct bond between the ligand with nonzero nuclear spin, in this case ^{17}O ($I = 5/2$), and iron. Thus, this result constitutes direct evidence for water ligand bound to the iron in the native and binary enzyme complexes. Furthermore, the dilution of ^{17}O water with ^{16}O water during sample preparation reduces the ^{17}O enrichment to approximately 53 atom %. Therefore, the maximal broadening due

(23) Ray, M.; Golombek, A. P.; Hendrich, M. P.; Yap, G. P. A.; Liable-Sands, L. M.; Rheingold, A. L.; Borovik, A. S. *Inorg. Chem.* **1999**, *38*, 3110−3115.
(24) Tocheva, E. I.; Rosell, F. I.; Mauk, A. G.; Murphy, M. E. P. *Science* **2004**, *304*, 867−870.

Table 2. Summary of EPR Data in ^{17}O-Enriched Water

enzyme sample	g	E:D	line width[a] (mT) $^{16}OH_2$	line width[a] (mT) $^{17}OH_2$	broadening[b] (mT)
cPAH−Fe•(NO)	4.08	0.011	3.8	4.2	0.4
	3.96		4.4	4.9	0.5
cPAH−Fe•($DMPH_4$)•(NO)	4.06	0.007	3.8	4.3	0.5
	3.98		4.4	4.9	0.5
cPAH−Fe•($DMPH_4$)•(Phe)•(NO)	4.27	0.044	4.8	4.7	−0.1
	3.76		7.3	7.4	0.1

[a] Measured as the full-width at half-height of the EPR resonance. [b] The difference between line widths in ^{17}O and ^{16}O water.

to ^{17}O hyperfine interaction is somewhat greater than that observed. In contrast, ternary complex cPAH−Fe•($DMPH_4$)•(Phe)•(NO) shows no broadening in ^{17}O water (Figure 3b and Table 2). Under the same conditions, the EPR spectrum of Fe^{II}(EDTA)(NO) is not broadened. These results provide direct evidence that in the ternary complex of cPAH, NO displaces a water ligand to afford a five-coordinate {Fe−NO}^{7} that does not contain an aqua ligand in the first coordination sphere (that is NO replaces the only water ligand in the ternary complex, Figure 2).

Electronic Spectroscopy and Thermodynamics of Iron Nitrosyl Formation. To further investigate the geometric changes observed by EPR spectroscopy, we acquired optical absorption spectra upon the addition of nitric oxide to ferrous cPAH−Fe in the presence or absence of substrates. The addition of nitric oxide to cPAH−Fe, cPAH−Fe•(Phe), and cPAH−Fe•($DMPH_4$) caused these solutions to become yellowish, as previously observed for nitrosyl adducts of other non-heme iron enzymes.[13−18] The spectra of cPAH−Fe•(NO) and cPAH−Fe•(Phe)•(NO) (Figure 4a, black and green dashed lines, respectively) exhibited a broad shoulder extending from 350 to 700 nm, though cPAH−Fe•(Phe)•(NO) possessed a slightly more pronounced shoulder from 400 to 500 nm. Interestingly, the addition of nitric oxide to the ternary complex of cPAH−Fe•($DMPH_4$)•(Phe) caused the solution to turn pink, and the resulting spectrum (Figure 4a, red dashed line) exhibited a well-defined peak at 440 nm and a more-intense shoulder between 500 and 600 nm than cPAH−Fe•(NO) and cPAH−Fe•(Phe)•(NO). Similar transitions for the non-heme iron nitrosyl model complex Fe(EDTA)(NO) studied by MCD and resonance Raman spectroscopy have been assigned as NO^--to-Fe^{3+} charge-transfer transitions, in which one transition at 575 nm (17 400 cm^{-1}) is due to the interaction of the in-plane (FeNO plane) NO^- $2\pi^*$ to Fe^{3+} $d_{x^2-y^2}$ orbitals, and two transitions at 509 (19 650 cm^{-1}) and 443 nm (22 580 cm^{-1}) are due to the in-plane NO^- $2\pi^*$ to Fe^{3+} d_{xz} and the out-of-plane NO^- $2\pi^*$ to Fe^{3+} d_{yz} transitions, respectively, with the latter transition being the most intense.[12] Because the strength of these transitions depend on the amount of overlap between the ligand and metal orbitals, the increase in intensity between 500 and 600 nm provides further support for NO binding at the W2 position, as the overlap between the in-plane $2\pi^*$ orbital with the $d_{x^2-y^2}$ and d_{xz} metal would be enhanced (Scheme 2). Alternatively, the sharpening of the spectrum for cPAH−Fe•($DMPH_4$)•(Phe)•(NO) may indicate a more-constrained binding site for the nitric oxide ligand to the metal center than for the cPAH−Fe•(NO) and cPAH−Fe•(Phe)•(NO) complexes. A similar interpretation was previously described by Hegg et al. for the change in the spectral features of the non-heme iron-containing enzyme TfdA upon addition of the α-ketoacid cofactor. The blue shift and increased sharpness of the spectrum for substrate-bound TfdA upon α-ketoacid addition was attributed to increased homogeneity of the iron environment, in which the Fe(II) became "locked" in position.[17] In the case of cPAH−Fe•($DMPH_4$)•(Phe)•(NO), the NO ligand may become locked in a position, which allows for greater overlap between the $2\pi^*$ and $d_{x^2-y^2}$, d_{xz}, and d_{yz} orbitals.

To determine if these spectral changes observed by EPR and optical spectroscopy influenced the ability of the Fe(II) center in cPAH to bind NO, we generated binding curves by monitoring the increase in absorbance of the charge-

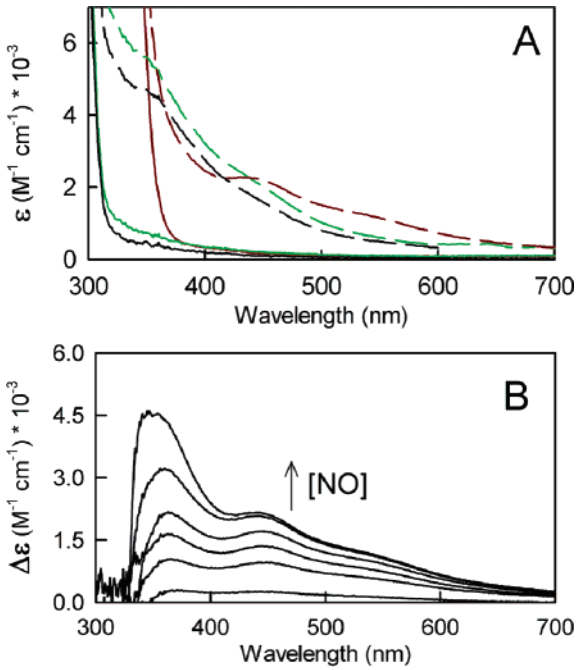

Figure 4. UV−visible absorption spectra of ferrous nitrosyl cPAH−Fe(II) complexes. (A) Spectra in the absence (solid lines) and presence (dashed lines) of nitric oxide of cPAH−Fe (black lines), cPAH−Fe•(Phe) (green lines), or cPAH−Fe•($DMPH_4$)•(Phe) (red lines). (B) Difference spectra of cPAH−Fe•($DMPH_4$)•(Phe) with initial NO concentration increasing from 10 to 200 μM (indicated by direction of arrow). Difference spectra = (spectra of cPAH−Fe•($DMPH_4$)•(Phe)•(NO)) − (spectrum of cPAH−Fe•($DMPH_4$)•(Phe)).

Scheme 2. Illustration of Enhancement of Ligand and Metal Orbital Overlap upon Rotation of NO Ligand

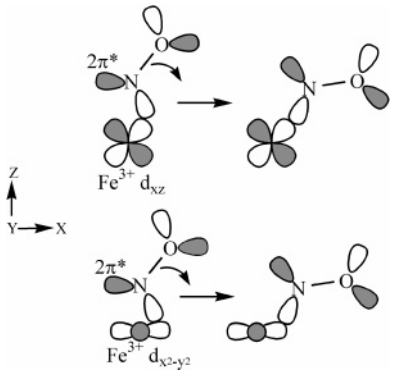

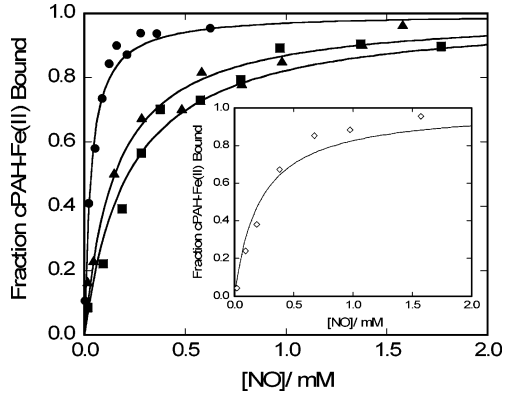

Figure 5. NO dissociation curves for cPAH−Fe•(NO) (◇, inset), cPAH−Fe•($DMPH_4$)•(NO) (▲), cPAH−Fe•(Phe)•(NO) (■), and cPAH−Fe•($DMPH_4$)•(Phe)•(NO) (●). The ordinate represents the fraction of cPAH−Fe bound by NO as determined by UV−visible spectroscopy. The abscissa represents the free (unbound) NO concentration, as calculated from the difference between the initial NO concentration added to the sample minus the concentration of NO-bound enzyme. Data points were fitted to the simple binding equation as follows: fraction of cPAH bound = [NO]/(K_d + [NO]), where K_d = dissociation constant.

transfer band at 440 nm for the cPAH−Fe complexes upon increasing NO concentrations. To diminish the light-scattering effects of the protein, we subtracted the spectrum of cPAH−Fe (or with appropriate substrates) in the absence of NO from the spectrum taken at each NO concentration. An example of the difference spectra for cPAH−Fe•($DMPH_4$)•(Phe)•(NO) is shown in Figure 4b, and the resulting binding curves for all the cPAH−Fe complexes are shown in Figure 5. The NO dissociation constants (K_d) were generated from a simple binding equation used to fit the data points (as described in the legend of Figure 5) and are listed in Table 1. cPAH−Fe•($DMPH_4$)•(Phe), with a K_d of 31 ± 2 μM, exhibited the highest affinity for NO binding, as its K_d value was approximately 5-fold smaller than the other complexes. cPAH−Fe and cPAH−Fe•(Phe) exhibited the lowest affinity for NO, with similar K_d values around 200 μM. These data support the published steady-state sequential binding order of cofactor, substrate, and finally oxygen, with the iron center preferentially binding the small diatomic molecule of NO (or O_2) only when both cofactor and substrate are present.[5] The K_d value for cPAH−Fe•($DMPH_4$)•(Phe)•(NO) compares favorably to the K_M value for O_2 (76 ± 7 μM) and provides further support for the use of NO as a mimic of oxygen.[5] Determinations of binding constants by EPR are in qualitative agreement with the observed trends from UV−vis measurements. However, at low NO concentrations (below 400 μM), integration of the small EPR signal was not reproducibly reliable enough to afford quantitative dissociation constants. It should be noted that for the EPR spectra reported, a concentration of 500 μM DEA/NO was employed, which yields [NO] = 750 μM, a value that is approximately 4× the highest K_d value observed for native enzyme cPAH−Fe•(NO) (Table 1). Thus, under these conditions, the majority of iron is NO-bound.

An increase in NO affinity in the presence of substrate has been previously measured for non-heme extradiol dioxygenases catechol 2,3-dioxygenase and protocatechuate 4,5-dioxygenase, both of which exhibit binding affinities 2 orders of magnitude higher in the presence of their respective catecholate substrates.[15] In comparison, the modest 5-fold increase exhibited by cPAH may reflect the difference in the NO-binding mechanism between the two types of enzymes. Whereas NO binds to the open-coordination site of the iron upon catecholate binding to the extradiol dioxygenases,[26] a water ligand (W2) on the iron center of cPAH must be displaced in order for the incoming NO molecule to bind. The increase in NO binding affinity for cPAH may represent the increased lability of the W2 ligand toward displacement in the presence of both substrate and cofactor.

Conclusion

We have presented evidence supporting the model in which nitric oxide (serving as an O_2 mimic) displaces the sole remaining water ligand on the iron center of the ternary complex of cPAH−Fe•($DMPH_4$)•(Phe) to yield a five-coordinate iron center. This result is in contrast with the mechanism of other non-heme iron enzymes, which direct oxygen binding to the open-coordination site on the iron center through the ligation of either substrate (e.g., isopenicillin N-synthase[25] and the extradiol dioxygenases[26]) or cofactor (e.g., α-ketoglutarate-dependent hydroxylase[17,27]) to the iron center. Because neither the cofactor nor the substrate for the pterin-dependent aromatic amino acid hydroxylases behave as iron ligands during catalysis, the site of oxygen binding appears to be controlled by second-coordination sphere effects, one of which may be the increased lability of the axial water ligand to displacement because of its unfavorable steric interaction with the bound phenyalanine substrate. The close positioning of the pterin cofactor to the open-coordination site may also serve to disfavor oxygen binding to this position.[10]

Acknowledgment. We are grateful to the NSF (Grants CHE-0434637 and CHE-0502391) for financial support, to Dr. Jon Fukuto for helpful discussions and insight, to Drs. Robert Taylor and Michael Everly for help with EPR experiments, and Dr. Christopher Switzer for help with the preparation of DEA/NO.

IC060478P

(25) Roach, P. L.; Clifton, I. J.; Hensgens, C. M. H.; Shibata, N.; Schofield, C. J.; Hajdu, J.; Baldwin, J. E. *Nature* **1997**, *387*, 827−830.
(26) Sato, N.; Uragami, Y.; Nishizaki, T.; Takahashi, Y.; Sazaki, G.; Sugimoto, K.; Nonaka, T.; Masai, E.; Fukuda, M.; Senda, T. *J. Mol. Biol.* **2002**, *321*, 621−636.
(27) Elkins, J. M.; Ryle, M. J.; Clifton, I. J.; Dunning Hotopp, J. C.; Lloyd, J. S.; Burzlaff, N. I.; Baldwin, J. E.; Hausinger, R. P.; Roach, P. L. *Biochemistry* **2002**, *41*, 5185−5192.